

# The quinoline bromoquinol exhibits broad-spectrum antifungal activity and induces oxidative stress and apoptosis in *Aspergillus fumigatus*

Dafna Ben Yaakov<sup>1</sup>, Yana Shadkchan<sup>1</sup>, Nathaniel Albert<sup>2</sup>, Dimitrios P. Kontoyiannis<sup>2</sup> and Nir Osherov<sup>1\*</sup>

<sup>1</sup>Department of Clinical Microbiology and Immunology, Sackler School of Medicine, Tel-Aviv University, Tel-Aviv, Israel; <sup>2</sup>Department of Infectious Diseases, Infection Control and Employee Health, University of Texas MD Anderson Cancer Center, Houston, TX, USA

\*Corresponding author. Tel: +972-3-640-9599; Fax: +972-3-640-9160; E-mail: nosherov@post.tau.ac.il

Received 26 December 2016; returned 1 March 2017; revised 8 March 2017; accepted 20 March 2017

**Objectives:** Over the last 30 years, the number of invasive fungal infections among immunosuppressed patients has increased significantly, while the number of effective systemic antifungal drugs remains low. The aim of this study was to identify and characterize antifungal compounds that inhibit fungus-specific metabolic pathways not conserved in humans.

**Methods:** We screened a diverse compound library for antifungal activity in the pathogenic mould *Aspergillus fumigatus*. We determined the *in vitro* activity of bromoquinol by MIC determination against a panel of fungi, bacteria and cell lines. The mode of action of bromoquinol was determined by screening an *Aspergillus nidulans* overexpression genomic library for resistance-conferring genes and by RNAseq analysis in *A. fumigatus*. *In vivo* efficacy was tested in *Galleria mellonella* and murine models of *A. fumigatus* infection.

**Results:** Screening of a diverse chemical library identified three compounds interfering with fungal iron utilization. The most potent, bromoquinol, shows potent wide-spectrum antifungal activity that was blocked in the presence of exogenous iron. Mode-of-action analysis revealed that overexpression of the *dba* secondary metabolite cluster gene *dbaD*, encoding a metabolite transporter, confers bromoquinol resistance in *A. nidulans*, possibly by efflux. RNAseq analysis and subsequent experimental validation revealed that bromoquinol induces oxidative stress and apoptosis in *A. fumigatus*. Bromoquinol significantly reduced mortality rates of *G. mellonella* infected with *A. fumigatus*, but was ineffective in a murine model of infection.

**Conclusions:** Bromoquinol is a promising antifungal candidate with a unique mode of action. Its activity is potentiated by iron starvation, as occurs during *in vivo* growth.

## Introduction

The incidence of life-threatening, invasive fungal infections has risen significantly during the past 30 years.<sup>1–3</sup> Most fungal infections are caused by species of *Cryptococcus*, *Candida* and *Aspergillus*.<sup>4</sup> It is estimated that invasive aspergillosis and candidiasis affect between 10% and 25% of all leukaemic and bone marrow transplant patients, with an alarmingly high mortality rate of ~50%.<sup>5,6</sup> However, despite the growing needs, treatments for invasive fungal infections remain unsatisfactory, with existing classes of antifungals showing toxicity, narrow specificity, increasing resistance or limited formulation.<sup>7</sup> Therefore, there is growing urgency to develop novel antifungals that inhibit fungus-specific targets.

We performed a novel screen of 40000 drug-like molecules from diverse chemical compound libraries, to identify antifungal compounds that inhibit specific fungal pathways not found in

humans. In particular, iron<sup>8</sup> and zinc<sup>9</sup> uptake, aromatic amino acid biosynthesis<sup>10</sup> and vitamin *para*-aminobenzoic acid (PABA),<sup>11</sup> riboflavin<sup>12</sup> and pyridoxine<sup>13</sup> biosynthesis pathways in fungi are of interest in antifungal drug discovery, as these pathways are not evolutionarily conserved in humans. We based our screen on the rationale that hit compounds inhibiting these pathways would be outcompeted and lose their activity upon supplementation with excess metal/aromatic amino acids/vitamins. We identified four compounds that lost all antifungal activity upon addition of excess iron or zinc, two compounds whose activity was eliminated by addition of riboflavin and one by addition of PABA. We focused on the most potent of these seven compounds, the quinoline bromoquinol, whose activity was blocked by iron, copper or zinc supplementation, suggesting that it interferes with the utilization of these essential metals. In this work, we describe the antifungal activity, selectivity, mode of action and *in vivo* activity of bromoquinol.

## Materials and methods

### Strains and media

The strains used in this study are detailed in Table S1 (available as Supplementary data at JAC Online). Moulds were grown in YAG yeast extract agar glucose medium or in defined minimal medium (MM) containing 70 mM NaNO<sub>3</sub>, 1% (w/v) glucose, 12 mM potassium phosphate pH 6.8, 4 mM MgSO<sub>4</sub> and 7 mM KCl as previously described.<sup>14</sup> Yeast was grown in YPD yeast peptone dextrose-rich medium and bacteria in LB broth.<sup>14</sup>

### Screen for antifungal compounds

*Aspergillus fumigatus* CEA10 was grown in 96-well plates in a volume of 100 µL of ΔMM [MM without Fe<sup>3+</sup>, Zn<sup>2+</sup>, PABA, pyridoxine, riboflavin and aromatic amino acids tryptophan (Trp), phenylalanine (Phe) and tyrosine (Tyr)] containing 5000 conidia. Each well was supplemented with 25 µM of compound from a chemical compound library ChemDiv Inc. (San Diego, CA, USA), TimeTec Chemicals (Hyderabad, India) and Asinex Ltd (Moscow, Russia) of 40000 compounds. MICs were determined after 48 h of incubation at 37°C, relative to the untreated control.

Next, each 'hit' was tested against a panel of 10 wells each containing a different additive: 100 µM Fe<sup>3+</sup>, 100 µM Zn<sup>2+</sup>, 500 µM PABA, 500 µM pyridoxine, 500 µM riboflavin, aromatic amino acids (0.01 mM Trp, 0.8 mM Tyr, 0.5 mM Phe), RPMI-MOPS medium lacking Fe<sup>3+</sup>, Zn<sup>2+</sup>, PABA, pyridoxine and riboflavin, or YAG. Compounds whose inhibitory activity was abolished upon addition of one of the additives mentioned above ('putative pathway inhibitors') were chosen for further evaluation.

### Pan-fungal and bacterial screen

The fungal strains listed in Table S1 were tested for susceptibility according to CLSI standard M27-A3 or M38-A2 protocols.<sup>15,16</sup> Bacterial strains (1.2 × 10<sup>6</sup> cfu/well) were grown in LB broth and MICs were determined after 48 h at 37°C at OD<sub>600</sub>.

### Cell culture

Hit compounds were tested for toxicity towards mammalian cells using the human lung epithelial cell line A549 (ATCC CLL 185) and NIH-3T3 mouse fibroblasts (ATCC CRL-1658) as described previously.<sup>14</sup> The XTT assay kit (Biological Industries, Beit Haemek, Israel) measured cell viability.

### Apoptosis assays and staining procedures

Fungal oxidative stress was detected by microscopy with the fluorescent dye dichlorofluorescein diacetate (DCFDA) according to the manufacturer's instructions (Abcam, San Francisco, CA, USA). For assessment of chromatin condensation by bromoquinol, nuclei were stained with DAPI. DNA-strand breaks were detected by terminal deoxynucleotidyl transferase dUTP nick-end labelling (TUNEL). Af293 protoplasts were prepared according to Jadoun et al.<sup>17</sup> Protoplasts were fixed in 4% paraformaldehyde solution and then incubated with permeabilization solution (0.1% Triton X-100, 0.1% sodium citrate) for 2 min on ice. Then, protoplasts were incubated with the TUNEL reaction mixture for 60 min at 37°C in the dark, according to the In Situ Cell Death Detection kit, Fluorescein (Roche Diagnostics, Germany). Microscopy was performed with a Zeiss Axio imager M1 fluorescence microscope. Images were captured with a Zeiss AxioCam MRm camera.

### Screening an *Aspergillus nidulans* overexpression genomic library for resistance-conferring plasmids

A library of *A. nidulans* transformants containing a genomic library cloned into the multicopy non-integrating vector pRG3-AMA1<sup>18,19</sup> was screened

for resistant strains. Transformation was undertaken as described previously.<sup>19</sup>

### RNAseq and RT-qPCR analysis

A detailed description of the RNAseq and RT-quantitative PCR (qPCR) analysis is provided in the Supplementary data. Primers used in this study are listed in Table S2.

### In vivo antifungal activity: *Galleria mellonella* model

Larvae were infected as previously described.<sup>14</sup> At 3 h post-infection, larvae were injected with 10 µL of saline containing bromoquinol. Larval survival was measured daily for up to 7 days post-treatment. This experiment was repeated twice with similar results.

### In vivo toxicity and antifungal activity: murine model

Female ICR mice (6 weeks old) were immunocompromised with cortisone acetate and infected intranasally with *A. fumigatus* Af293 conidia as previously described.<sup>20</sup> Mice were treated by intraperitoneal injection 2 h post-inoculation and then once a day for two consecutive days. Viability was assessed for 2 weeks. This experiment was repeated twice with similar results. Experiments were ethically approved by the Ministry of Health Animal Welfare Committee, Israel.

## Results

To identify antifungal compounds, we screened 40000 drug-like molecules from diverse chemical compound libraries of small molecular weight compounds. Each compound (at a concentration of 25 µM) was tested for antifungal activity against a patient isolate of *A. fumigatus* (CEA10), in a 96-well based liquid assay in ΔMM for 48 h of incubation at 37°C. ΔMM is defined as MM lacking supplementation with Fe<sup>3+</sup>, Zn<sup>2+</sup>, PABA, pyridoxine, riboflavin and aromatic amino acids (Trp, Tyr, Phe). Fungal growth on this medium appeared phenotypically normal and growth was reduced by only 20% compared with that of standard supplemented MM as assessed by dry weight of the lyophilized mycelium suggesting they contain traces of Fe<sup>3+</sup> and Zn<sup>2+</sup> capable of supporting growth. The wells were screened by an inverted light microscope. We identified 237 compounds that completely inhibited germination (MIC ≤ 25 µM) and selected them for further analysis. We added Fe<sup>3+</sup>, Zn<sup>2+</sup>, PABA, pyridoxine, riboflavin or the aromatic amino acids (Trp, Tyr, Phe) to *A. fumigatus* in the presence of each of the 237 inhibitory compounds at 25 µM. We identified seven inhibitors for which addition of iron (bromoquinol, C11-375, B11-375, D2-431), PABA (D2-77) or riboflavin (G8-58, D4-65) completely reversed inhibition (Table 1 and Figure S1 for chemical structures). Of these seven inhibitors we chose to focus on the quinoline bromoquinol, because of its low MIC (1 µM) in both ΔMM and RPMI-MOPS without Fe<sup>3+</sup>, Zn<sup>2+</sup>, PABA, pyridoxine and riboflavin, its clearly defined abolishment of activity in the presence of Fe<sup>3+</sup> to the medium (Figure 1) and its non-toxicity towards cells in culture at these concentrations (Table 2).

### Antifungal activity spectrum of the quinoline bromoquinol

We tested bromoquinol activity on a wide range of pathogenic fungal strains, mammalian cell lines and bacteria in culture

**Table 1.** MICs of 'hits' from *A. fumigatus* screen

Activity blocked by	$\Delta$ MM	+Fe <sup>3+</sup> 100 $\mu$ M	+Zn <sup>2+</sup> 100 $\mu$ M	+PABA 50 $\mu$ M	+Pyroxidine 50 $\mu$ M	+Riboflavin 50 $\mu$ M	+Aromatic amino acids <sup>a</sup>	$\Delta$ RPMI-MOPS <sup>b</sup>	YAG <sup>c</sup>
Iron									
bromoquinol	1	>25	>25	1	1	1	1	1	>25
C11-375	6.25	>25	>25	6.25	6.25	6.25	6.25	6.25	>25
B11-375	25	>25	25	25	25	25	25	25	>25
D2-431	25	>25	25	25	25	25	25	25	>25
PABA									
D2-77	25	25	25	>25	25	25	25	>25	>25
Riboflavin									
G8-59	25	25	25	25	25	>25	25	>25	>25
D4-65	25	25	25	25	25	>25	25	25	>25

<sup>a</sup>Trp (0.01 mM), Tyr (0.8 mM), Phe (0.5 mM).

<sup>b</sup>RPMI-MOPS without Fe<sup>3+</sup>, Zn<sup>2+</sup>, PABA, pyroxidine and riboflavin.

<sup>c</sup>YAG = rich fungal medium.

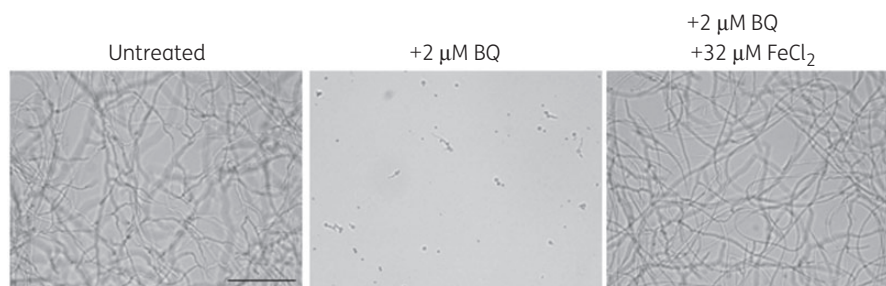


**Figure 1.** Antifungal activity of bromoquinol is abolished by iron. *A. fumigatus* conidia were grown for 24 h at 37 °C in MM lacking iron. Addition of 2  $\mu$ M bromoquinol completely inhibited fungal growth. Supplementation with 32  $\mu$ M FeCl<sub>2</sub> blocked the antifungal activity of bromoquinol. BQ, bromoquinol.

(Table 2). Bromoquinol was effective against *A. fumigatus* spp. (0.06 < MIC < 1  $\mu$ M) and *Candida* spp. (1 < MIC < 4  $\mu$ M). Zygomycetes (*Rhizopus* species) were less susceptible with MICs of 16–32  $\mu$ M or higher after 48 h. Bromoquinol only weakly inhibited NIH-3T3 (by 20%) and A549 cell (by 10%) proliferation at 25  $\mu$ M, measured with the XTT cell viability assay. These data show that bromoquinol was much more potent at inhibiting fungal growth as compared with mammalian cell lines. The bacterial strains were weakly susceptible to bromoquinol, with MIC values of 12.5 or 25  $\mu$ M, indicating that it was not entirely fungus specific. We tested the fungicidal activity of bromoquinol against *A. fumigatus* Af293 and *Candida albicans* CBS562. Bromoquinol achieved 95% killing at 8  $\mu$ M in *A. fumigatus* (minimal fungicidal concentration 32  $\mu$ M) and in *C. albicans* 99% killing at 1  $\mu$ M (minimal fungicidal concentration 1  $\mu$ M). Bromoquinol did not cause haemolysis of sheep red blood cells after 24 h at a concentration of 25  $\mu$ M, indicating that it does not act as a non-specific membrane-disrupting agent (data not shown).

### Bromoquinol activity is abolished by addition of Fe<sup>3+</sup>, Cu<sup>2+</sup> or Zn

We tested the effect of increasing iron concentrations on growth inhibition (MIC) of *A. fumigatus* (Af293), *A. nidulans* (R153) and

*C. albicans* (CBS562) by bromoquinol (Table 3). Addition of iron to MM lacking iron at concentrations between 2 and 32  $\mu$ M gradually abolished growth inhibition by bromoquinol. In all three fungi, this effect was already evident at 2–8  $\mu$ M of iron indicating that bromoquinol acts in a similar manner. Further analysis in *A. fumigatus* (Af293) demonstrated that increased levels of the metals zinc and copper at similar concentrations also abolished inhibition by bromoquinol (Tables S3 and S4). Addition of a strong chelator of Cu<sup>2+</sup> (bathocuprine disulfonic acid) or Fe<sup>3+</sup> (triacetyl fusarinine) restored bromoquinol inhibition in the presence of excess copper or iron addition, demonstrating that Fe<sup>3+</sup>/Cu<sup>2+</sup> inactivation of bromoquinol is reversible (Tables S5 and S6).

### Structure–activity relationships of related quinolines

We carried out a structure–activity relationship analysis of three commercially available quinolines in comparison with bromoquinol. MICs were determined for *A. fumigatus* Af293 grown for 48 h on RPMI-MOPS (Table 4). Replacement of the Br residues at positions 5 and 6 in bromoquinol with Cl (in dichloro 8-hydroxyquinoline) or I and Cl (in 5-chloro-7-iodo-8-hydroxyquinoline/clioquinol) did not improve antifungal activity (MIC 1  $\mu$ M for all three compounds). Removal of the halogenated residues at these positions (in 8-hydroxyquinoline) strongly reduced activity (MIC 32  $\mu$ M).

**Table 2.** MICs of bromoquinol for pathogenic fungal strains, bacteria and mammalian cell lines

Species (no. of strains tested)	MIC <sup>a</sup> (μM)
<i>A. fumigatus</i> (12)	0.06–1
<i>Aspergillus flavus</i> (7)	1–2
<i>Aspergillus niger</i> (5)	0.5–1
<i>Aspergillus terreus</i> (5)	2–4
<i>Rhizopus oryzae</i> (6)	16 to >32
<i>Candida glabrata</i> (3)	2
<i>Candida tropicalis</i> (1)	2
<i>Candida krusei</i> (5)	2–4
<i>C. albicans</i> (4)	1–2
<i>Candida parapsilosis</i> (5)	1–4
<i>Candida rugosa</i> (2)	2–4
<i>Saccharomyces cerevisiae</i> (2)	1–2
<i>Escherichia coli</i> (1)	25
<i>Staphylococcus epidermidis</i> (1)	12.5
<i>Staphylococcus aureus</i> (1)	25
<i>Bacillus cereus</i> (1)	12.5
A549	>25 (10%) <sup>b</sup>
NIH-3T3	>25 (20%) <sup>b</sup>

<sup>a</sup>MIC = the lowest drug concentration completely to arrest germination and growth after 48 h at 37 °C. Fungal strains were grown in RPMI-MOPS (moulds) or in YPD (yeast), mammalian cell lines were grown in DMEM supplemented with 10% FCS and bacteria were grown in LB broth.

<sup>b</sup>MIC (cell culture) = % growth inhibition at 25 μM bromoquinol, as measured by the XTT assay.

Addition of iron or zinc strongly reduced the antifungal activity of all of the quinolines tested. Interestingly, whereas addition of copper strongly reduced the antifungal activity of the halogenated quinolines, it strongly increased the activity of 8-hydroxyquinoline (MIC – Cu<sup>2+</sup> = 32 μM, MIC + Cu<sup>2+</sup> = 2 μM).

### Screening an *A. nidulans* overexpression genomic library for resistance-conferring plasmids

To identify the molecular target of bromoquinol, we screened a multicopy non-integrating genomic library of *A. nidulans* based on the high copy vector pRG3-AMA1.<sup>19</sup> Conidia (5×10<sup>4</sup>/mL) of the library were plated under bromoquinol (8–10 μM) selection in MM without iron. After 6 days at 37 °C, five resistant colonies were identified and the multicopy library vector from all transformants was isolated. These plasmids were transformed once more into *A. nidulans* via transformation by protoplasting<sup>21</sup> and one of them conferred resistance to bromoquinol and two other halogenated quinolines, but not to 8-hydroxyquinoline or the antifungals caspofungin, voriconazole or amphotericin B (Table 5). Sequencing of the plasmid revealed that it contained three genes, *dbaA* (AN7896), *dbaB* (AN7897) and *dbaD* (AN7898), composing part of a secondary metabolite cluster. To identify which of these genes conferred bromoquinol resistance, we used transposon mutagenesis mapping. We searched for single insertions that caused the *A. nidulans* resistant strain to lose resistance to bromoquinol upon transformation, as this is expected to occur in the rescuing gene.

**Table 3.** Effect of different Fe<sup>3+</sup> concentrations on MICs of bromoquinol for *A. fumigatus*, *A. nidulans* and *C. albicans*

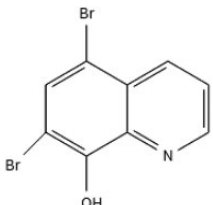
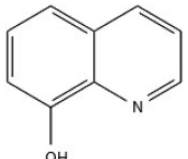
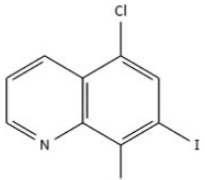
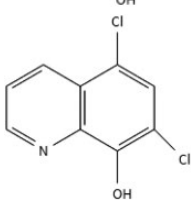
Fe <sup>3+</sup> concentration (μM)	MIC (μM) for <i>A. fumigatus</i> (Af293)	MIC (μM) for <i>A. nidulans</i> (R153)	MIC (μM) for <i>C. albicans</i> (ATCC 2901)
0	1	0.5	1
2	2	4	2
4	8	8	2
8	8	32	4
16	16	32	16
32	32	>32	32
64	32	>32	>32
128	>32	>32	>32

Sequencing of the area bordering the single transposon insertion revealed that resistance-inactivating insertions occurred separately in two of the three genes: *dbaA* and *dbaD*. These genes are both members of the *dba* secondary metabolite gene cluster. The putative cluster spans 12 genes in total. Of the 12 genes, *dbaA* encodes a Zn(II)2Cys6 transcription factor with a role in activating the cluster and *dbaD* encodes a major facilitator superfamily (MFS) transporter with a possible role in secreting the secondary metabolite made by the cluster.<sup>22</sup> We propose that overexpression of the *DbaD* transporter may confer resistance to the halogenated quinolines by specifically increasing their efflux (see the Discussion section).

### Bromoquinol activates genes involved in oxidation-reduction, efflux and secondary metabolite clusters

To gain further insight into the mode of action of bromoquinol, we performed RNAseq analysis of *A. fumigatus* cells exposed to the compound (see Supplementary data for experimental details). *A. fumigatus* (Af293) conidia were germinated in MM without iron for 16 h at 37 °C and treated with 2 μM bromoquinol for 1 h. The mycelium was harvested, total RNA prepared and used to generate cDNA libraries that were sequenced with the Illumina HiSeq2000 instrument. Differential expression analysis revealed 8800 expressed genes (87% of the genes in the *A. fumigatus* genome). Bromoquinol treatment increased the expression of 1025 genes by >2-fold. Of these, 906 annotated genes were evaluated by GO/gene ontology term enrichment analysis. Significantly enriched up-regulated gene categories included secondary metabolite clusters ( $P=7.8\times 10^{-20}$ ), transporters ( $P=4.9\times 10^{-13}$ ) and genes involved in oxidation-reduction ( $P=3.7\times 10^{-19}$ ) (Table 6 and Table S7). Up-regulated transporters included 51 MFS and 11 ABC transporters and among them two homologues of the *dbaD* transporter (*Afu3g03320*, *Afu1g05170*) identified above in *A. nidulans* as conferring bromoquinol resistance. However, this transcriptional activation does not lead to resistance, as this requires expression from multiple copies of the gene as seen in *A. nidulans*. Interestingly genes from 14 of the 31 secondary metabolite clusters found in *A. fumigatus* were up-regulated by bromoquinol, including the gliotoxin, NRPS1, fumigalavine C and trypacidin clusters. Up-regulated genes involved in

**Table 4.** MIC ( $\mu\text{M}$ ) values of different quinolines for *A. fumigatus*

Compound name	Structure	MIC (–iron)	MIC (+iron <sup>a</sup> )	MIC (+zinc <sup>b</sup> )	MIC (+copper <sup>c</sup> )
Bromoquinol		1	>32	32	32
8-Hydroxyquinoline		32	>32	>32	2
5-Chloro-7-iodo-8-hydroxyquinoline (clioquinol)		1	>32	8	16
5,7-Dichloro-8-hydroxyquinoline		1	16	16	16

<sup>a</sup>Iron ( $\text{FeCl}_2$ ) = 64  $\mu\text{M}$ .

<sup>b</sup>Zinc ( $\text{ZnSO}_4$ ) = 64  $\mu\text{M}$ .

<sup>c</sup>Copper ( $\text{CuSO}_4$ ) = 3  $\mu\text{M}$ .

**Table 5.** MICs of quinolines and antifungals for resistant *A. nidulans* An-AMA *pdbaA/B/D* and control An-AMA strains

	Bromoquinol ( $\mu\text{M}$ )	5-Chloro-7-iodo-8-quinolinol ( $\mu\text{M}$ )	5,7-Dichloro-8-hydroxyquinoline ( $\mu\text{M}$ )	8-Hydroxyquinoline ( $\mu\text{M}$ )	Voriconazole (mg/L)	Caspofungin (mg/L)	Amphotericin B (mg/L)
An-AMA <sup>a</sup>	1	0.5	1	16	0.125	0.125 <sup>b</sup>	1
An-AMA <i>pdbaA/B/D</i>	2	2	4	32	0.125	0.125 <sup>b</sup>	1

<sup>a</sup>Control *A. nidulans* strain containing the empty AMA cloning vector.

<sup>b</sup>MEC values.

oxidation–reduction included 20 glutathione *S*-transferase genes that encode proteins that can detoxify  $\text{H}_2\text{O}_2$ , 20 cytochrome P450 oxidoreductases and 16 FAD-dependent oxidoreductases, suggesting that the fungus is experiencing oxidative stress. Notably two putative pro-apoptotic genes (*Afu3g01290*, *Afu2g00230*) with homology to yeast apoptosis inducing factor were also activated.

Significantly enriched down-regulated gene categories most notably included genes involved in ribosome biogenesis ( $P=1.1\times 10^{-81}$ ) and among them many genes encoding

translation initiation factors, ribosomal proteins and ribosomal RNA processing and assembly factors (Table 6 and Table S7).

We used RT-qPCR to analyse the mRNA levels of five key genes showing up-regulation after RNA sequencing, following exposure to bromoquinol compared with untreated Af293. The RT-qPCR analysis validated the results of the RNAseq, including up-regulation of the two *A. fumigatus dbaD* homologues *Afu3g03320* and *Afu1g05170* (Table 7 and Supplementary data).

Taken together, the transcriptional profile indicated that after exposure to bromoquinol, *A. fumigatus* drastically reduced



energy-consuming cellular activities and in particular protein synthesis. It activated a large number of genes apparently involved in drug efflux and detoxification of bromoquinol and in response to reactive radical formation.

### Bromoquinol induces oxidative stress and apoptosis in *A. fumigatus*

Based on the RNAseq results showing significant activation of glutathione *S*-transferase genes and oxidoreductases after bromoquinol treatment, we directly assayed the cells for oxidative stress. We used the fluorescent dye DCFDA that measures reactive oxygen species within the cell. *A. fumigatus* (Af293) hyphae treated for 1 h with 10  $\mu$ M bromoquinol in the presence of DCFDA fluoresced to an extent similar to that following treatment with the known reactive oxygen species stressor menadione, indicating that bromoquinol strongly induced oxidative stress (Figure 2a). Because oxidative stress is a strong activator of apoptotic cell death, we carried out two independent assays to evaluate if bromoquinol-treated *A. fumigatus* hyphae underwent apoptosis. Fungal apoptosis, determined by nuclear DAPI staining, revealed extensive chromatin condensation and fragmentation in *A. fumigatus* treated for 2 h with 10  $\mu$ M bromoquinol, similar in extent to the apoptosis induced by H<sub>2</sub>O<sub>2</sub> treatment (Figure 2b). The detection of apoptosis-induced DNA strand breaks by TUNEL showed that protoplasts treated with 10  $\mu$ M bromoquinol for 2 h at 37°C exhibited nuclear fluorescence indicative of double-strand break formation similar to that shown by treatment with 0.1 mM H<sub>2</sub>O<sub>2</sub> (Figure 2c). In

**Table 6.** Selected enriched up-regulated and down-regulated genes in *A. fumigatus* in response to bromoquinol

Category	<i>n</i>	<i>P</i>
Up-regulated genes		
secondary metabolite clusters	56	7.2E–20
transporters	74	4.9E–13
oxidation–reduction	121	3.7E–19
Down-regulated genes		
ribosome biogenesis	120	1.1E–81
nitrogen compound metabolism	168	2.4E–26
primary metabolic process	367	1.1E–16

**Table 7.** RNAseq validation of key bromoquinol up-regulated genes

Gene	Description	RNAseq		RT-qPCR	
		fold change	<i>P</i>	fold change	SD
<i>Afu3g03320</i>	MFS monocarboxylate transporter <i>dbaD</i> homologue	13	2.77E–16	36	0.7
<i>Afu1g05170</i>	MFS monocarboxylate transporter <i>dbaD</i> homologue	3.9	2.39E–23	3.2	1.2
<i>Afu3g01400</i>	ABC multidrug transporter	19.5	1.71E–99	126	1.3
<i>Afu3g01290</i>	AMID-like mitochondrial oxidoreductase	14.6	2.04E–15	93	1.3
<i>Afu4g14530</i>	glutathione <i>S</i> -transferase <i>Ure2</i> -like	16	1.33E–19	70	0.1

summary, these results indicate that bromoquinol induces rapid oxidative stress and apoptosis in *A. fumigatus*.

### Bromoquinol reduces mortality in *G. mellonella* larvae infected with *A. fumigatus*

To evaluate the efficacy of bromoquinol in treating invasive aspergillosis, we used the *G. mellonella* infection model. Infected larvae were injected with bromoquinol at different concentrations (ranging from 4 to 8 mg/kg) or with 2 mg/kg amphotericin B as a positive treatment control (Figure 3a). Bromoquinol was not effective at a concentration of 4 mg/kg (*P* = 0.43; 4 mg/kg 20% survival after 7 days), but showed efficacy at 8 mg/kg (*P* = 0.0024; 60% survival after 7 days) similar to that of the proven antifungal amphotericin B (*P* < 0.0001; 60% survival after 7 days).

### Bromoquinol is ineffective in a murine model of invasive pulmonary aspergillosis

Mice were immunosuppressed with cortisone acetate and infected by intranasal inoculation with *A. fumigatus* conidia. Treatment was performed by intraperitoneal injection 2 h after infection and on the next two consecutive days. Survival in each group (*n* = 10) was monitored over 14 days. Whereas the control antifungal amphotericin B significantly reduced mortality (*P* = 0.004; 50% mortality after 14 days), treatment with bromoquinol at 3 mg/kg (*P* = 0.34) or 8 mg/kg (*P* = 0.43) was ineffective (Figure 3b).

## Discussion

### A novel antifungal screen identified compounds interfering with key virulence-associated metabolic pathways in *A. fumigatus*

We performed a novel screen of small molecular drug-like compounds to identify inhibitors that specifically interfere with unique fungal pathways (iron uptake, vitamin pathways, aromatic amino acid synthesis) not found in humans and essential for virulence.<sup>8–11,13</sup> We focused on the study of bromoquinol because it was highly potent (at low micromolar concentrations) in the absence of iron, and lost all activity upon addition of iron. We found that bromoquinol is fungus-specific *in vitro* and active in an insect model of infection, but ineffective in a murine model of invasive pulmonary aspergillosis. The lack of bromoquinol activity in the latter model might have several explanations, such as bromoquinol binding by serum, rapid rate of clearance and limited penetration

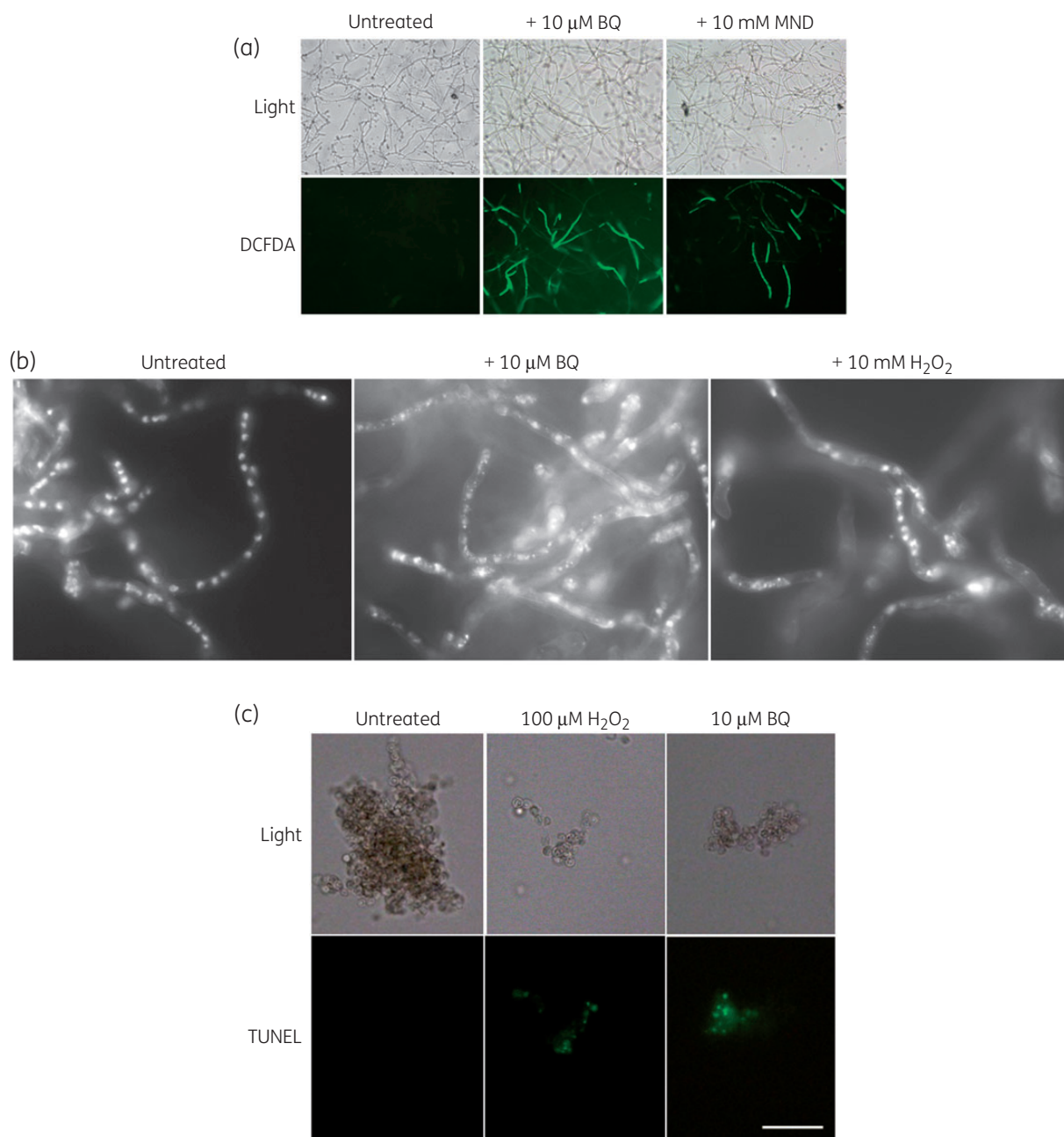


**Figure 2.** Bromoquinol induces oxidative stress and apoptosis in *A. fumigatus*. *A. fumigatus* conidia were grown for 16 h at 37 °C. Addition of 10 μM bromoquinol-induced (a) oxidative stress as measured by DCFDA fluorescence. (b) Nuclear DNA fragmentation and (c) TUNEL DNA double-strand break formation in protoplasts, both characteristic of fungal apoptosis. BQ, bromoquinol, H<sub>2</sub>O<sub>2</sub>, a known inducer of apoptosis; MND, menadione, a known inducer of oxidative stress. This figure appears in colour in the online version of JAC and in black and white in the print version of JAC.

into the infected lungs. Further optimization and study of the pharmacokinetics/pharmacodynamics of bromoquinol in the murine model is needed.

Importantly, bromoquinol would have probably been discarded in a standard screen because it is a weak antifungal in most fungal media that contain iron at high micromolar levels. This is an example of drug discovery that capitalizes on the important environmental cues of *in vivo* growth, specifically the conditions of scarcity of essential elements such as iron.

### **Bromoquinol exhibits divalent metal-dependent antifungal activity *in vitro* and *in vivo***

Bromoquinol is a brominated derivative of the agricultural fungicide and antimicrobial 8-hydroxyquinoline.<sup>23</sup> 8-Hydroxyquinoline forms weak to moderate affinity complexes with divalent metal ions such as zinc, copper and iron. Therefore, it was suggested that 8-hydroxyquinoline acts in fungi by chelating metals, such as zinc, copper and iron, and inhibiting cellular metal-dependent

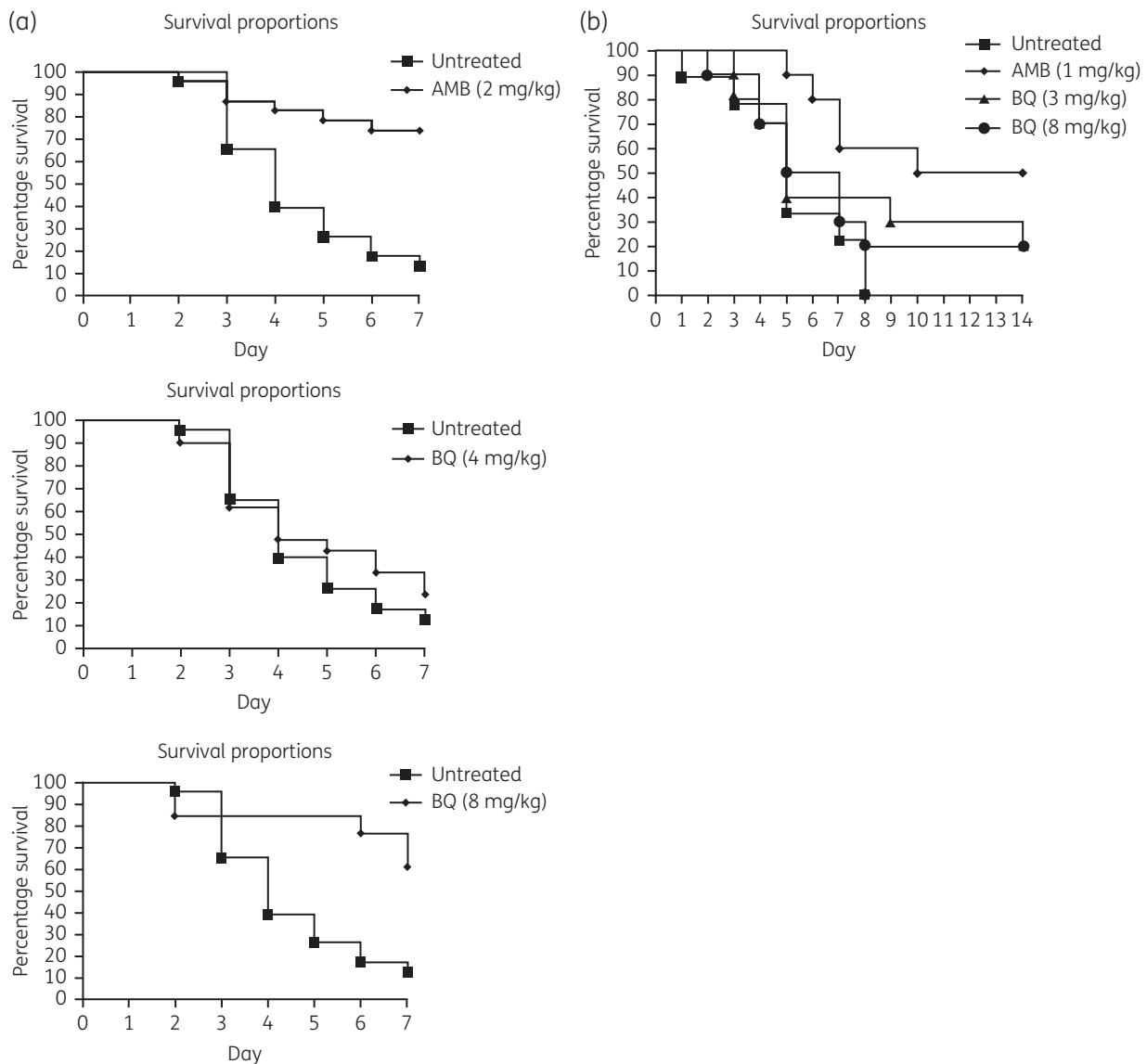


**Figure 3.** Bromoquinol reduces mortality in *G. mellonella* larvae infected with *A. fumigatus*. (a) Bromoquinol at a concentration of 8 mg/kg significantly ( $P=0.0024$ ) reduced mortality of *Galleria* larvae injected with  $5 \times 10^5$  conidia of *A. fumigatus*. (b) Bromoquinol at a concentration of up to 8 mg/kg did not reduce mortality in immunosuppressed mice inoculated intranasally with  $5 \times 10^5$  conidia of *A. fumigatus*. Antifungal amphotericin B was used as a positive treatment control. AMB, amphotericin B; BQ, bromoquinol.

catalysis.<sup>24</sup> Clioquinol (5-chloro-7-iodo-8-hydroxyquinoline), in addition to antimicrobial activity, showed efficacy in mouse models of Alzheimer's, Parkinson's and Huntington's disease.<sup>25</sup> The *in vitro* activity of bromoquinol against pathogenic yeasts was recently demonstrated, but its mode of action was not described.<sup>26</sup>

### **Resistance to bromoquinol in *A. nidulans* is conferred by overexpression of *dbaD* encoding a secondary metabolite cluster transporter**

We performed a library screen for bromoquinol resistance genes in *A. nidulans* and found that overexpression of *dbaA* (AN7896) and

*dbaD* (AN7898) conferred resistance to bromoquinol. The *dbaA* and *dbaD* null strains,<sup>22</sup> however, showed WT susceptibility to bromoquinol (data not shown), suggesting that in these strains additional efflux mechanisms had been activated.

*dbaA* and *dbaD* are members of the *A. nidulans* *dba* gene cluster, containing 12 genes in total, involved in the synthesis of the secondary metabolite 2,4-dihydroxy-3-methyl-6-(2-oxopropyl)benzaldehyde, that has antibacterial activity and is an intermediate in the production of the azaphilones, antimicrobial yellow pigments.<sup>22</sup> *dbaA* encodes a Zn(II)<sub>2</sub>Cys<sub>6</sub> transcription factor that activates the *dba* cluster and *dbaD* encodes an MFS transporter that is proposed to transport the metabolites produced by the cluster, into the environment.<sup>22</sup>



We showed that the two *A. fumigatus dbaD* homologues *Afu3g03320* and *Afu1g05170* are also up-regulated in response to bromoquinol. Interestingly, based on our analysis of published transcriptome datasets, these two genes are not up-regulated in response to the conventional antifungals caspofungin, voriconazole and amphotericin B,<sup>27–29</sup> but are strongly up-regulated under hypoxia<sup>30</sup> and haem starvation (Hubertus Haas, personal communication). This suggests that activation of the *dba* cluster may be partly controlled by the transcription factor *SrbA* that controls the hypoxic response, which includes activation of haem biosynthesis.<sup>31</sup> Taken together, our findings suggest that overexpression of the *dbaA* transcription factor and *dbaD* transporter could result in increased efflux of bromoquinol from the fungal cell and therefore increased resistance, although this needs to be rigorously assessed by measuring the efflux of radioactively-labelled bromoquinol. This finding is conceptually important because it suggests that secondary metabolite cluster efflux transporters, in addition to secreting secondary metabolites, can also be co-opted to rid the cell of toxic compounds found in its environment, including antifungal compounds.

### Proposed mode of action of bromoquinol

Bromoquinol functions as an inducible antifungal. In the presence of iron, copper or zinc, bromoquinol is chelated and inactive. Under conditions of low concentrations of these metals, as found in the infected host, active bromoquinol monomers are released. The bromoquinol monomers inside the fungal cell bind to iron, copper or zinc coordinated into the active site of metalloenzymes, and in particular oxidoreductases.<sup>24</sup> This interferes with their catalytic functions, disrupting the redox potential of the cell and inducing oxidative stress leading to apoptosis and cell death as shown in the Results section. An alternative model, in which bromoquinol acts by chelating intracellular metals, can be discarded for several reasons, e.g. (i) most fungi, including *A. fumigatus* possess endogenous metal chelators such as siderophores with much higher affinities than bromoquinol, and (ii) the RNAseq analysis provides no evidence that bromoquinol induces the expression of genes associated with metal starvation.

### Conclusions

In conclusion, bromoquinol presents novel opportunities for the development of inducible antifungals. Future directions include generating bromoquinol derivatives conjugated to existing antifungals that will dissociate and act under the low iron/copper/zinc concentrations found in fungus-infected tissue.

### Acknowledgements

We would like to thank Gilgi Freidlander for performing the bioinformatics analysis of the RNAseq data, Hubertus Haas for kindly providing us with triacetyl fusarinine and for useful discussions and Amir Sharon for his help in the apoptosis analysis.

### Funding

This study was supported by The Binational Science Foundation (BSF) 2011322 grant to N. O. and D. P. K.

### Transparency declarations

None to declare.

### Supplementary data

Supplementary methods, Tables S1 to S7 and Figure S1 are available as Supplementary data at JAC Online (<http://jac.oxfordjournals.org/>).

### References

- Ben-Ami R, Lewis RE, Kontoyiannis DP. Invasive mould infections in the setting of hematopoietic cell transplantation: current trends and new challenges. *Curr Opin Infect Dis* 2009; **22**: 376–84.
- Yapar N. Epidemiology and risk factors for invasive candidiasis. *Ther Clin Risk Manag* 2014; **10**: 95–105.
- Lewis RE, Cahyame-Zuniga L, Leventakos K et al. Epidemiology and sites of involvement of invasive fungal infections in patients with haematological malignancies: a 20-year autopsy study. *Mycoses* 2013; **56**: 638–45.
- Brown GD, Denning DW, Gow NA et al. Hidden killers: human fungal infections. *Sci Transl Med* 2012; **4**: 165rv13.
- Denning DW. Early diagnosis of invasive aspergillosis. *Lancet* 2000; **355**: 423–4.
- Groll AH, Shah PM, Mentzel C et al. Trends in the postmortem epidemiology of invasive fungal infections at a university hospital. *J Infect* 1996; **33**: 23–32.
- Paiva JA, Pereira JM. New antifungal antibiotics. *Curr Opin Infect Dis* 2013; **26**: 168–74.
- Haas H. Iron—a key nexus in the virulence of *Aspergillus fumigatus*. *Front Microbiol* 2012; **3**: 28.
- Wilson D, Citiulo F, Hube B. Zinc exploitation by pathogenic fungi. *PLoS Pathog* 2012; **8**: e1003034.
- Sasse A, Hamer SN, Amich J et al. Mutant characterization and in vivo conditional repression identify aromatic amino acid biosynthesis to be essential for *Aspergillus fumigatus* virulence. *Virulence* 2016; **7**: 56–62.
- Brown JS, Aufauvre-Brown A, Brown J et al. Signature-tagged and directed mutagenesis identify PABA synthetase as essential for *Aspergillus fumigatus* pathogenicity. *Mol Microbiol* 2000; **36**: 1371–80.
- Becker JM, Kauffman SJ, Hauser M et al. Pathway analysis of *Candida albicans* survival and virulence determinants in a murine infection model. *Proc Natl Acad Sci USA* 2010; **107**: 22044–9.
- Purnell DM. The effects of specific auxotrophic mutations on the virulence of *Aspergillus nidulans* for mice. *Mycopathol Mycol Appl* 1973; **50**: 195–203.
- Mircus G, Albert N, Ben-Yaakov D et al. Identification and characterization of a novel family of selective antifungal compounds (CANBEFs) that interfere with fungal protein synthesis. *Antimicrob Agents Chemother* 2015; **59**: 5631–40.
- Clinical and Laboratory Standards Institute. *Reference Method for Broth Dilution Antifungal Susceptibility Testing of Filamentous Fungi—Second Edition: Approved Standard M38-A2*. CLSI, Wayne, PA, USA, 2008.
- Clinical and Laboratory Standards Institute. *Reference Method for Broth Dilution Antifungal Testing of Yeasts—Third Edition: Approved Standard M27-A3*. CLSI, Wayne, PA, USA, 2008.
- Jadoun J, Shadkhan Y, Oshero N. Disruption of the *Aspergillus fumigatus argB* gene using a novel in vitro transposon-based mutagenesis approach. *Curr Genet* 2004; **45**: 235–41.
- Oshero N, Mathew J, May GS. Polarity-defective mutants of *Aspergillus nidulans*. *Fungal Genet Biol* 2000; **31**: 181–8.
- Oshero N, May G. Conidial germination in *Aspergillus nidulans* requires RAS signaling and protein synthesis. *Genetics* 2000; **155**: 647–56.

- 20** Vaknin Y, Hillmann F, Iannitti R et al. Identification and characterization of a novel *Aspergillus fumigatus* rhomboid family putative protease, RbdA, involved in hypoxia sensing and virulence. *Infect Immun* 2016; **84**: 1866–78.
- 21** Osmani SA, May GS, Morris NR. Regulation of the mRNA levels of *nimA*, a gene required for the G2-M transition in *Aspergillus nidulans*. *J Cell Biol* 1987; **104**: 1495–504.
- 22** Gerke J, Bayram O, Feussner K et al. Breaking the silence: protein stabilization uncovers silenced biosynthetic gene clusters in the fungus *Aspergillus nidulans*. *Appl Environ Microbiol* 2012; **78**: 8234–44.
- 23** Prachayasittikul V, Prachayasittikul S, Ruchirawat S et al. 8-Hydroxyquinolines: a review of their metal chelating properties and medicinal applications. *Drug Des Devel Ther* 2013; **7**: 1157–78.
- 24** Nicoletti G, Domalewski E, Borland R. Fungitoxicity of oxine and copper oxinate: activity spectrum, development of resistance and synergy. *Mycol Res* 1999; **103**: 1073–84.
- 25** Bareggi SR, Cornelli U. Clioquinol: review of its mechanisms of action and clinical uses in neurodegenerative disorders. *CNS Neurosci Ther* 2012; **18**: 41–6.
- 26** Zuo R, Garrison AT, Basak A et al. In vitro antifungal and antibiofilm activities of halogenated quinoline analogues against *Candida albicans* and *Cryptococcus neoformans*. *Int J Antimicrob Agents* 2016; **48**: 208–11.
- 27** Altwasser R, Baldin C, Weber J et al. Network modeling reveals cross talk of MAP kinases during adaptation to caspofungin stress in *Aspergillus fumigatus*. *PLoS One* 2015; **10**: e0136932.
- 28** da Silva Ferreira ME, Malavazi I, Savoldi M et al. Transcriptome analysis of *Aspergillus fumigatus* exposed to voriconazole. *Curr Genet* 2006; **50**: 32–44.
- 29** Gautam P, Shankar J, Madan T et al. Proteomic and transcriptomic analysis of *Aspergillus fumigatus* on exposure to amphotericin B. *Antimicrob Agents Chemother* 2008; **52**: 4220–7.
- 30** Losada L, Barker BM, Pakala S et al. Large-scale transcriptional response to hypoxia in *Aspergillus fumigatus* observed using RNAseq identifies a novel hypoxia regulated ncRNA. *Mycopathologia* 2014; **178**: 331–9.
- 31** Blatzer M, Barker BM, Willger SD et al. SREBP coordinates iron and ergosterol homeostasis to mediate triazole drug and hypoxia responses in the human fungal pathogen *Aspergillus fumigatus*. *PLoS Genet* 2011; **7**: e1002374.